Ultrasound Image Segmentation of Brachial Plexus Nerves using UNet integrated with Tsallis Entropy

Submitted in partial fulfillment of the requirements

of the degree of

BACHELOR OF TECHNOLOGY

By

Ashutosh Kumar (177208)

Saurav Verma (177258)

Shivansh Dubey (177260)

Supervisor

Dr. K. V. Kadambari

Department of Computer Science and Engineering

National Institute of Technology, Warangal –

506004

INDIA, June 2021

APPROVAL SHEET

This Project Work entitled **Ultrasound Image Segmentation of Brachial Plexus Nerves using UNet integrated with Tsallis Entropy** by **Ashutosh Kumar, Saurav Verma and Shivansh Dubey** is approved for the degree of Bachelor of Technology in Computer Science and Engineering at National Institute of Technology, Warangal during the year 2020-21.

Examiners

_____

_____

_____

_____

_____

Supervisor

_____

Dr. K. V. Kadambari

Assistant Professor, CSE Dept.

Chairman

_____

Prof. P Radha Krishna

Head of Department, CSE

NIT Warangal

Date :_____

Place :_____

DECLARATION

We declare that this written submission represents our ideas in our own words and where others' ideas or words have been included, we have adequately cited and referenced the original sources. We also declare that we have adhered to all principles of academic honesty and integrity and have not misrepresented or fabricated or falsified any idea/ data/ fact/ source in our submission. We understand that any violation of the above will be cause for disciplinary action by the Institute and can also evoke penal action from the sources which have thus not been properly cited or from whom proper permission has not been taken when needed.

_____

(Signature)

Ashutosh Kumar

177208

Date: _____

_____

(Signature)

Saurav Verma

177258

Date: _____

_____

(Signature)

Shivansh Dubey

177260

Date: _____

NATIONAL INSTITUTE OF TECHNOLOGY WARANGAL

DEPARTMENT OF COMPUTER SCIENCE AND ENGINEERING

CERTIFICATE

This is to certify that the project work entitled "**Ultrasound Image Segmentation of Brachial Plexus Nerves using UNet integrated with Tsallis Entropy**" is a bonafide record of work carried out by by Ashutosh Kumar (177208), Saurav Verma (177258) and Shivansh Dubey (177260), submitted to the faculty of Computer Science and Engineering Department, in partial fulfillment of the requirements for the award of the degree of Bachelor of Technology in Computer Science and Engineering at National Institute of Technology, Warangal during the academic year 2020-2021.

Dr. K. V. Kadambari	Prof. P Radha Krishna
Project Guide	Head of the Department
Department of CSE	Department of CSE
NIT Warangal	NIT Warangal

ACKNOWLEDGEMENT

We consider it as a great privilege to express our deep gratitude to many respected personalities who guided, inspired and helped us in the successful completion of this project.

We would like to express our deepest gratitude to our guide, Dr. K. V. Kadambari, Department of Computer Science and Engineering, National Institute of Technology, Warangal, for her constant supervision, suggestions, guidance and invaluable encouragement during this project. She has been a constant source of inspiration and helped us in each stage.

We are grateful to Prof. P Radha Krishna, Head of the Department, Computer Science and Engineering, National Institute of Technology, Warangal for his constant moral support to carry out this project.

We are very thankful to the Project Evaluation Committee, for their strenuous efforts to evaluate our projects.

We wish to thank all the staff members in the department for their kind cooperation and support given throughout our project work. We are also thankful to our parents, family and all our friends who have given valuable suggestions and help in all stages of the development of the project.

Ashutosh Kumar (177208)
Saurav Verma (177258)
Shivansh Dubey (177260)

ABSTRACT

Ultrasound Guided Regional Anesthesia (UGRA) is one of the most prevalent practices of administering anesthesia to the nerves that help reduce risk of nerve block and trauma complications. Many years of experience is required by an anesthesiologist to identify nerves from ultrasound images, which are often contaminated with speckle noise and motion artefacts, before applying anesthesia to the region. Automating the process of identifying the nerve sites by image segmentation of ultrasound scans would

benefit the development of UGRA practices and reduce the risks associated with regional anesthesia treatments. In this paper we present an information entropy-based feature pooling of the nerve images. The medical dataset is often either small or intermixed with noise and false positives. Our method introduces the concept of Tsallis entropy-based feature pooling to improve accuracy of the pre-existing UNet model on the dataset. The system is tested on a 20 percent test split of our Ultrasound images dataset. Experiment showed a significantly better performance in terms of accuracy and dice score when compared to the base UNet architecture.

LIST OF FIGURES

LIST OF TABLES

Contents

Chapter 1

Introduction

Ultrasound Guided Regional Anesthesia (UGRA) is an anesthetic procedure involving locating a certain nerve block site using Ultrasound images for guidance. Traditionally anesthesiologists used to inject the needle without any visualization leading to an increase in surgery failures and nerve traumas [leave this for reference]. UGRA practices reduced these risks but they are still not put into use very often primarily because of the extensive experience overhead required by the anesthesiologists. Moreover, the ultrasound images are of low contrast - low intensity nature as compared to their CT and MRI counterparts. Any of the above factors can contribute to improper administration of anesthesia leading to several pre- and post-surgery complications ranging from anesthetic toxicity, epileptic seizures to central nervous system depression and even coma.

However, given the fact many hospitals in developing countries neither have dedicated trauma centers nor enough resources for high resolution image scanning, image segmentation can find great application in such scenarios.

Image segmentation focuses on pixel wise labelling of different object categories. In medical segmentation, this indicates separation of dominant background class from smaller Region of Interest (ROI) class i.e. binary segmentation. But the class imbalance can lead to false negatives from the dataset. Other issues of medical segmentation are scarcity and poor quality of data. Speckle noise introduced in the US during the image formation results in a granular texture in the images which reduces the overall SNR [2], [4]. Moreover, because the US images are hypo-echoic, the nerve region is not a salient structure in the images. Identifying the nerve contour amongst other anatomical features such as bone, muscle or blood vessels is very challenging [1], [5]. In addition to accurate ROI localization, the US segmentation practices must also minimize the likelihood of false positives as it could have adverse effects on the patient, making US segmentation a complicated problem to solve.

Amidst the above-mentioned scenarios, it becomes very important to achieve good segmentation performance despite the flaws in the dataset. This work focuses on the operation of the UNet model and introduces Tsallis Entropy in the domain of feature-based pooling to the original model.

Chapter 2

Problem Statement

To study and analyze the concept of UNet architecture and Tsallis Entropy in order to build an efficient deep learning model and then compare the model performance with base UNet model on Ultrasound images dataset using a suitable cost metric.

Accuracy of predicted mask images holds a great significance especially in medical image segmentation. Even a minor improvement in accuracy can increase the overall usefulness of the model in the medical field. For this purpose, any factor that can hamper the training of model should be targeted and tried to be mitigated. Therefore, our aim is to focus on diminishing the distraction created by noise with the help of Tsallis Entropy based Pooling Technique working within the model. This will improve the training rate and in turn will yield a better accuracy in the predicted masks.

Chapter 3

Review of Literature

Various approaches have been used for the detection and segmentation of brachial plexus in their corresponding Ultrasound images and have produced a variety of results on different performance metrics.

Prior to the era of deep learning, edge-based learning, texture-based and deformable models have been used for image segmentation. Then came Convolutional Neural Networks (CNNs) which achieved great success in image classifications. However, in biomedical segmentation applications, the output is expected to be a pixel-wise class probability map to detect the ROIs.

The first Fully Connected Neural Network was realized by Long et al. in 2015[8] which was later modified into UNet by Ronneberger et al. [7] in 2015. This model followed a symmetric encoder- decoder structure where the encode half mimics a CNN with sequential convolution, activation and max pooling layers and the decoder half consist of a series of up-sampling layers that would reconstruct a segmented image. Later a connection was introduced between the encoder and decoder feature maps to propagate contextual information to the higher resolution layers. As a result, the U-Net is able to localize high level-features and output a probability map that contains contextual information similar to the input image. Due to its simple architecture UNet soon gained popularity in the medical image segmentation field.

Kakade et al. [1] proposes an improvement to the framework which includes feature selection, feature extraction, and segmentation where the authors apply textural based preprocessing and PCA based post-processing on the US images and predicted output masks respectively to refine the anatomical contours, and create contiguous segmentation maps. This is later realized as a vanilla UNet architecture. Using the same data set as [1], Baby et al. introduces a set of feature extraction and feature selection prior to segmentation with U-Net [5] , where the images are pre-processed by histogram equalization, adjusted using morphological reconstruction, and then smoothed using a non-linear adaptive filter. Using the same US data set as [1] and [5], Li et al. [9] uses a U-Net with noisy activation functions to improve the segmentation performance in the presence of speckle noise.

Other versions of UNet find their application on different US datasets such as cardiac, breast and fetal images. Azzopardi et al. proposes a phased congruence map of the cardiac US images in the Fourier domain [10]. These maps are theoretically invariant to any noise and hence the segmentation mask produced should be equally unaffected by the said noise.

In another study by Cerrolaza et al. [12] the authors have used a 2 Stage CNN model (2S-CNN) for fetal skull US images where the architecture incorporates contextual and structural information into the segmentation process, whereas Zhang et al. [13] propose a FCN using a faster R-CNN architecture to achieve localization of ROI in the poor image quality.

Our work is loosely based on the hybrid approaches of [10], [11] and [12]. However, we incorporate the use of Entropy based pooling to deal with the noise and other irrelevant features of our low-quality US image dataset.

Chapter 4

Intuition

Datasets have always been a major limitation when it comes to medical image segmentation. An ordinary human can perform a classification operation on images fairly easily when compared to any advanced neural network model. However, in scenarios such as performing manual image segmentation we can only rely on the highly trained experts that have field experience. Even after that the resultant masks are prone to human errors such as false positives and negatives. Hence gathering a reliable dataset with all images appropriately labelled especially in the medical field becomes a major challenge.

It is understood that UNet like any other image segmentation model tries to identify a repeating pattern in the dataset while training and adjusts its knowledge accordingly. However the dataset for our work is also loaded with speckle noise that can hamper the learning ability of UNet. It can make UNet learn unnecessary features (also called distractions) and in turn hamper the segmentation process resulting in inaccurate and false image masks. Hence aiding the UNet by alerting it of the distractions created by noise seems to be the need of the hour.

This is where the concept of Entropy Based Pooling comes in. Entropy is a thermodynamic concept that defines the randomness or unpredictability in any system. Higher Entropy value is associated with higher randomness of the system. Since noise and other such errors contribute to higher randomness, they lead to higher entropy value regions in our image. Hence assisting the UNet model with entropy values of different regions in the image and forcing the model to

ignore regions of higher entropy(noise) can help in faster convergence and better performance of the model.

Chapter 5

Formulas Used

5.1 Overview of UNet Architecture

UNet was originally invented for biomedical image segmentation. It is claimed to perform well especially for cases with small datasets. UNet architecture is a symmetric encoder-decoder system. Unlike classification, image segmentation requires labelling operation at pixel level as well as a mechanism to learn various distinctive features at different stages of learning.

The basic overview of UNet architecture is:

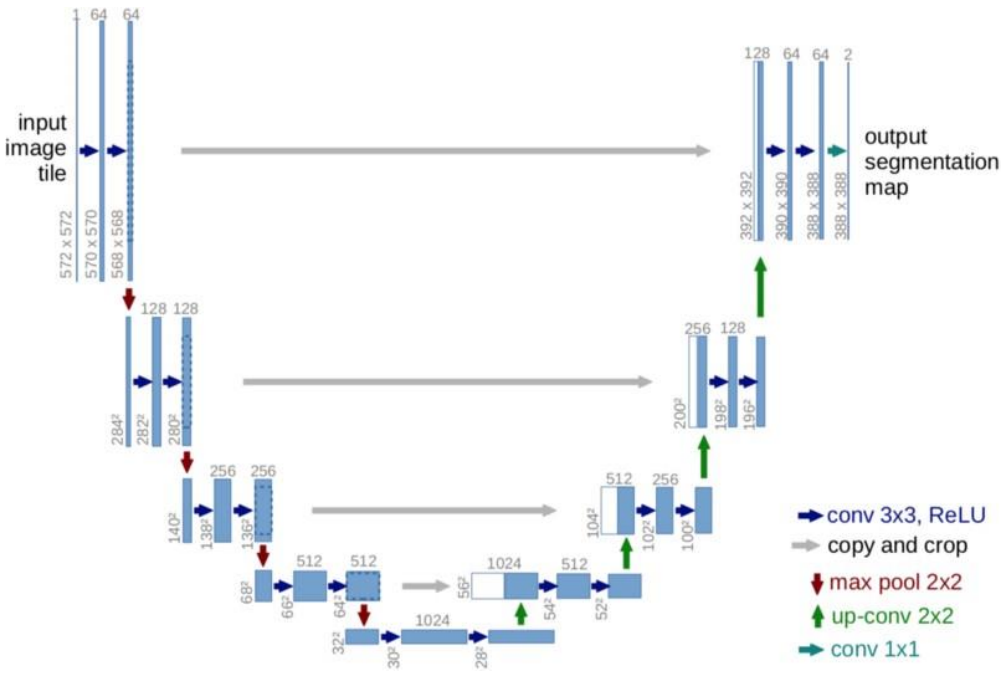

Figure 5.1: Architecture of a standard UNet

• **Encoder half**:

This part is also called down sampling where the pixel resolution of images decreases and the number of channels (or feature maps) increases. This is done to do away with the huge number of pixel values that the model had to handle otherwise while retaining all the major and minor relevant features without any significant loss. This idea is achieved via a series of convolution and max pooling block laid in a sequence with a few activation functions laid in between the layers. This path followed is often called 'contracting path' which looks like:

conv_layer1 -> conv_layer2 -> max_pooling -> dropout(optional)

which matches with:

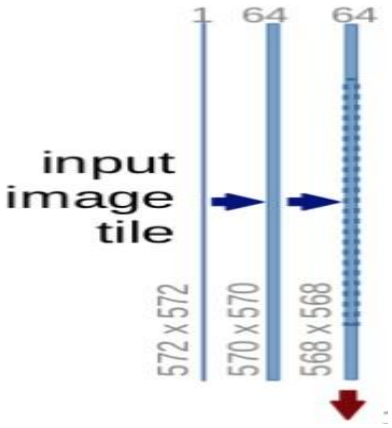

Figure 5.2: Single layer of UNet Encoder half

This is repeated at least 3 times to get the resolution which is:

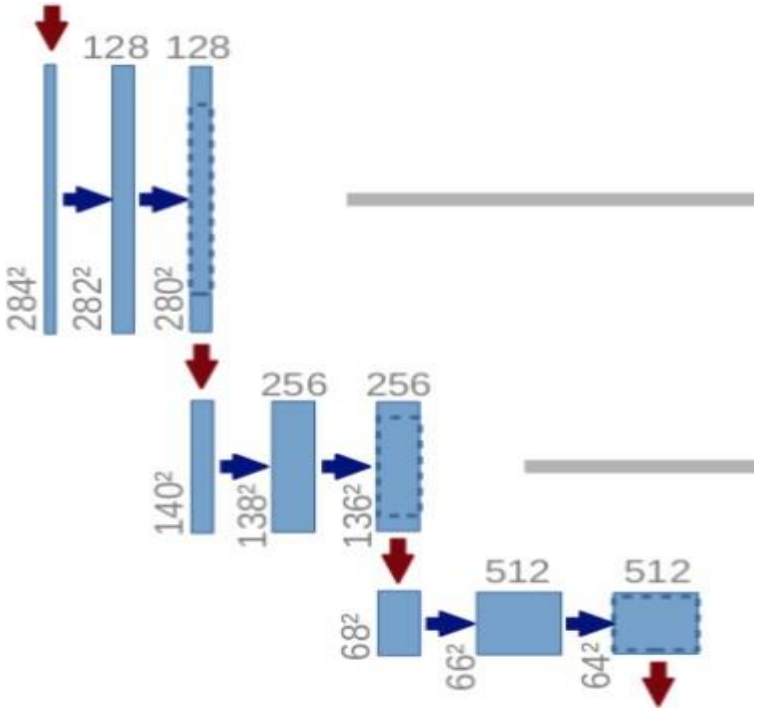

Figure 5.3: Encoder half of a UNet

Hence one can easily relate this half of the UNet with a pre-trained classification network like VGG/ResNet.

- **Decoder half**:

Also known as the up-sampling half or the path of expansion. The intuition behind this layer is that after the encoder layer any and all discriminative features learnt have to be transferred onto the pixel space and hence the condensed feature map has to be expanded to the original dimension as that of the masked image. This idea is achieved simply by applying sequential layers of up sampling and concatenation followed by regular convolution operation which looks like:

```
conv_2d_transpose -> concatenate -> conv_layer1 -> conv_layer2
```

and matches with:

Figure 5.4: Single Layer of UNet Decoder half

5.2 Tsallis Entropy

The Concept of Entropy is derived from Albuquerque et al [6], which showed the effect of entropy when introduced into sub-extensive and super-extensive system.

From thermodynamic point of view, Entropy is defined as the measure of randomness or unpredictability of a system. Since the amount of noise in an image dataset is directly proportional to the randomness, an increase in noise in an image region therefore increases the entropy of that region. One of the most common form of entropy is the Boltzmann/Gibbs Entropy (BGS) in which the entropy of a discrete source is often obtained from the probability distribution, where $p = \{p_i\}$ is the probability of finding the system in each possible state *i.*

Therefore, $0 \leq p_i \leq 1$ and $\sum^k p_i = 1$, where k is the total number of states. The Shannon entropy may be described as:

$$S = \sum_{i=1}^{k} p_i \, ln(p_i) \ . \quad (1)$$

This formulism seems to be applicable only to the system that follow Gibbs Statistics that is a system where microscopic interactions and microscopic memory are short ranged. Statistically if we take two independent sub systems A and B , the probability of composite system is $p^{A+B} = p^A p^B$ or in terms of entropy, the system follows additive property that is: $S(A + B) = S(A) + S(B)$. Because of the above requirement that Gibbs Entropy demand from the system it fails to be useful for systems where microscopic interactions and microscopic memory are long ranged for e.g. the US dataset that our work is based on.

Hence, we require a more universal form of entropy, one which can be applied to any form of system without changing the base concept. This is where Tsallis entropy is proven to be useful. The general formula of Tsallis Entropy is defined as:

$$S_q = \frac{1 - \sum_{i=1}^{k} (p_i)^q}{q-1}, \quad (2)$$

where k is the total number of possibilities of the system and q is a real number also known as entropic index that characterizes the degree of non-extensivity. This expression meets the BGS entropy in the limit $q \rightarrow 1$. The Tsallis Entropy is non extensive in such a way that for two statistically independent subsystem A and B the total entropy will be calculated as

$$S_{q.}(A+B) = S_{q.}(A) + S_{q.}(B) + (q-1).S_{q.}(A).S_{q.}(B). \quad (3)$$

Depending on the value of entropic index in equation (3), any system can be divided into three categories. They are:

1. Sub extensive system (q<1): $S_{q.}(A+B) < S_{q.}(A) + S_{q.}(B)$
2. Extensive system (q=1): $S_{q.}(A+B) = S_{q.}(A) + S_{q.}(B)$
3. Super extensive system (q>1): $S_{q.}(A+B) > S_{q.}(A) + S_{q.}(B)$

Chapter 6

Design and Implementation

In this project two models are compared side by side. They are:

1. Base UNet Model
2. Tsallis-UNet Model

Base UNet model is going to have a similar architecture to that of UNet discussed in section(?). However, this UNet is specially modified to run on low powered CPUs to reduce overhead issues.

On the other hand Tsllis-Unet model is the main model on which the entire project is based upon. The details of each are discussed in further sections.

6.1 Dataset

Publicly available dataset of Ultrasound images of Brachial Plexus nerve is used. These images were first made available on Kaggle as a part of Nerve Segmentation Challenge in 2016. The Dataset consist of training set and testing set.

The Training set has around 5635 ultrasound images. Each of these images has a annotated mask which shows if the said image has any Brachial Plexus nerve present in them. If the nerves are

present they are shown via a white ROI in a black background else the mask is left completely black. Annotations were done by a group of trained experts who marked the ROI in the images if they believed them to contain the nerve. However, this make data more prone to chances of false positive and negatives.

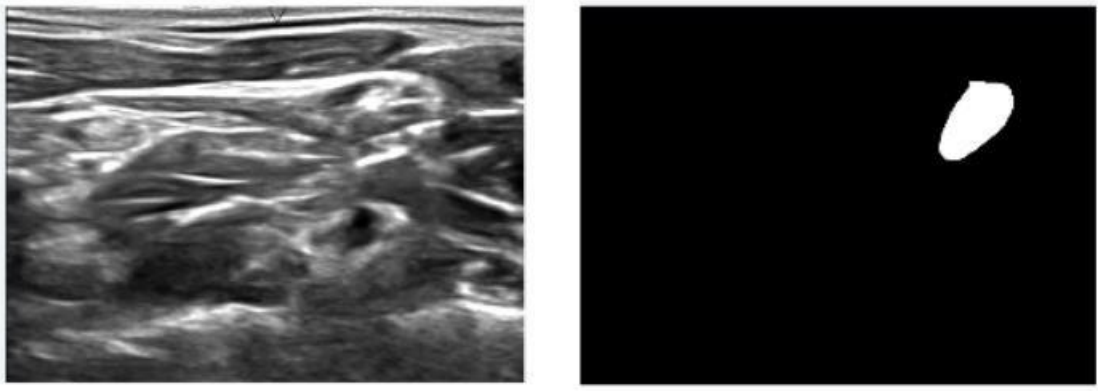

Figure 6.1: Left: Ultrasound image of Brachial Plexus Nerves of a patient. Right: Annotated ROI for image denoting the location of Brachial Plexus Nerves

The Testing set has around 5508 ultrasound images. However, none of them have any mask image that could have been used to test the accuracy of our model. As this dataset is insufficient to generate any test score or loss value, it will be only used to generate predicted masks once our models are completely trained.

Hence for training of our model we will use Training set itself. The dataset will be divided into 80:20 ratio where the first half will be used to train the model and later 20% will be used to check for validation. For each model this dataset will be divided into 32 batches and will be run for 20 epochs.

6.2 Data Preprocessing

During pre-processing the US images in the training set are resized to 96 x 96 and mean centered

with a standard deviation of 1. As the image masks are of low contrast, this resizing of US images is done to allow the images to fit into the memory and increase training convergence by improving the gradient flow. This will also reduce the computational overhead on the system CPUs.

Apart from the above pre-processing, a training label is also created for each of the masked image. This is done for the second model that is Tsallis UNet. Each of these training labels will be 0-1 hot encoded based on the absence or presence of Brachial Plexus in the ROI respectively.

6.3 Model A: Base-UNet Model

As explained earlier in section 5.1, UNet is specifically designed to run well for various medical image segmentation. The UNet in this project also called Base UNet is loosely based on that of Abraham et al. []. The modifications have been done keeping in mind the sheer size of Training set and limited processing capability of system CPU.

This model has 5 layers in the encoding half. Each Layer begins with two successive Convolutions with 3 x 3 sliding window and ReLu activation followed by Max Pooling to reduce the feature map size by half. In [Abraham et al] Max pooling was replaced with Average Pooling to get better results. However, we have switched back to Max Pooling and now a Dropout is introduced which follows each of these Max Pooling to ensure that model doesn't overfit.

After the convolution layer comes 5 layers of decoder half. This half is used to reconstruct a predicted mask image. Each layer begins with a Transpose of 2 x 2 sliding window. It is followed by two successive Convolution and a Dropout similar to that in encoder.

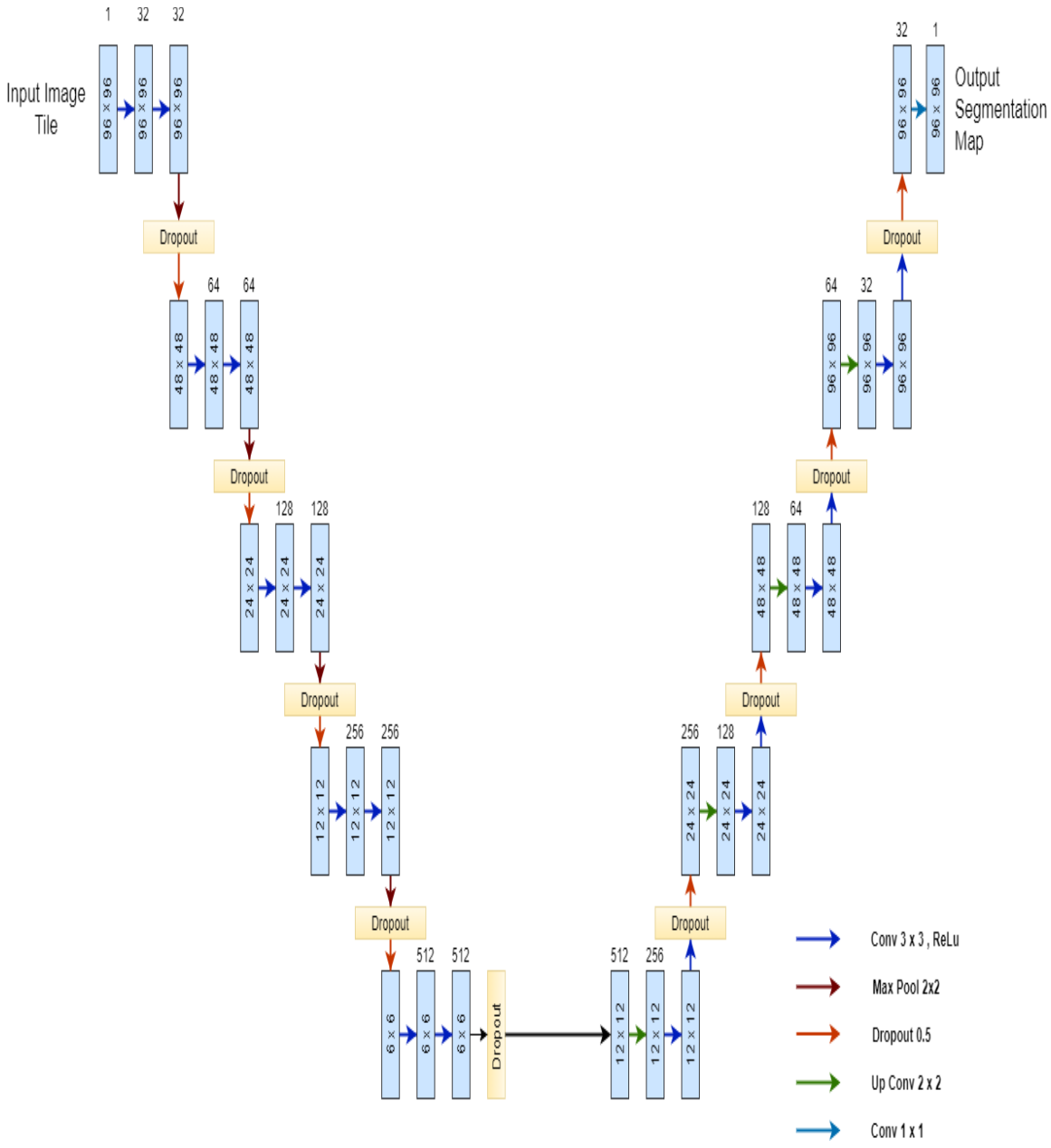

Figure 6.2: Proposed Architecture for the Base-UNet model

6.4 Model B: Tsallis-UNet Model

This model is implemented on top of the Base-UNet (Model A).

Tsallis Entropy suppresses the noise to a great extent. However, a major challenge that we face is

its integration to an image segmentation model. Tsallis is generally used for image classification where the resulting entropy pooling is fed into a dense net while predicting a certain classification result. However, as we know that image segmentation is classification of each pixel rather than the entire image, theoretically Tsallis entropy can still be integrated with model A as the background remains the same.

In any version of UNet the weights deciding the classification of each pixel (or segmentation of the image) lies dominatingly in the encoder half. During the training of UNet any error that the model learns is used to readjust these weights. Therefore, it is wise to make sure that it is these weights that are trained to not get distracted by the noise. This is where Tsallis Entropy finds its application.

What we have proposed is a two-header approach. This model is a single input two output model. Input to this model is same as that for the Base UNet. The combine learning from both pipelines will be used to readjust the weights of encoder half. This way Tsallis UNet makes use of Tsallis Entropy to ignore the noise without losing its basic UNet structure.

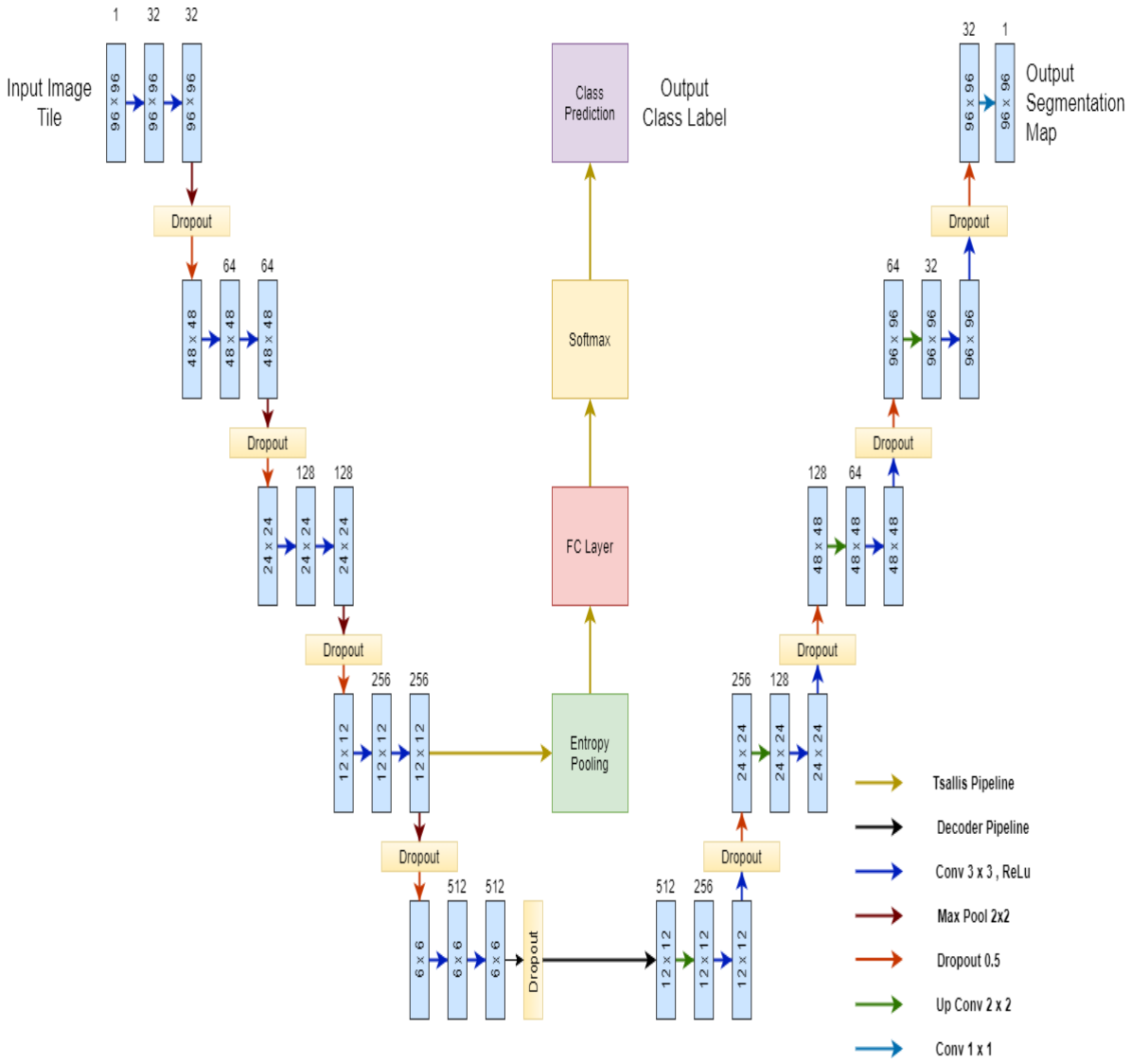

Figure 6.3: Proposed Architecture for the Tsallis-UNet –
single input multiple output model

6.4.1 Decoder Pipeline

This half is the same as that in the Base UNet. It begins right after the 5th layer of encoder where information regarding pixel-wise classification is transferred to first layer of the Decoder. This half reconstructs a predicted mask which is then compared to the corresponding mask of the training set.

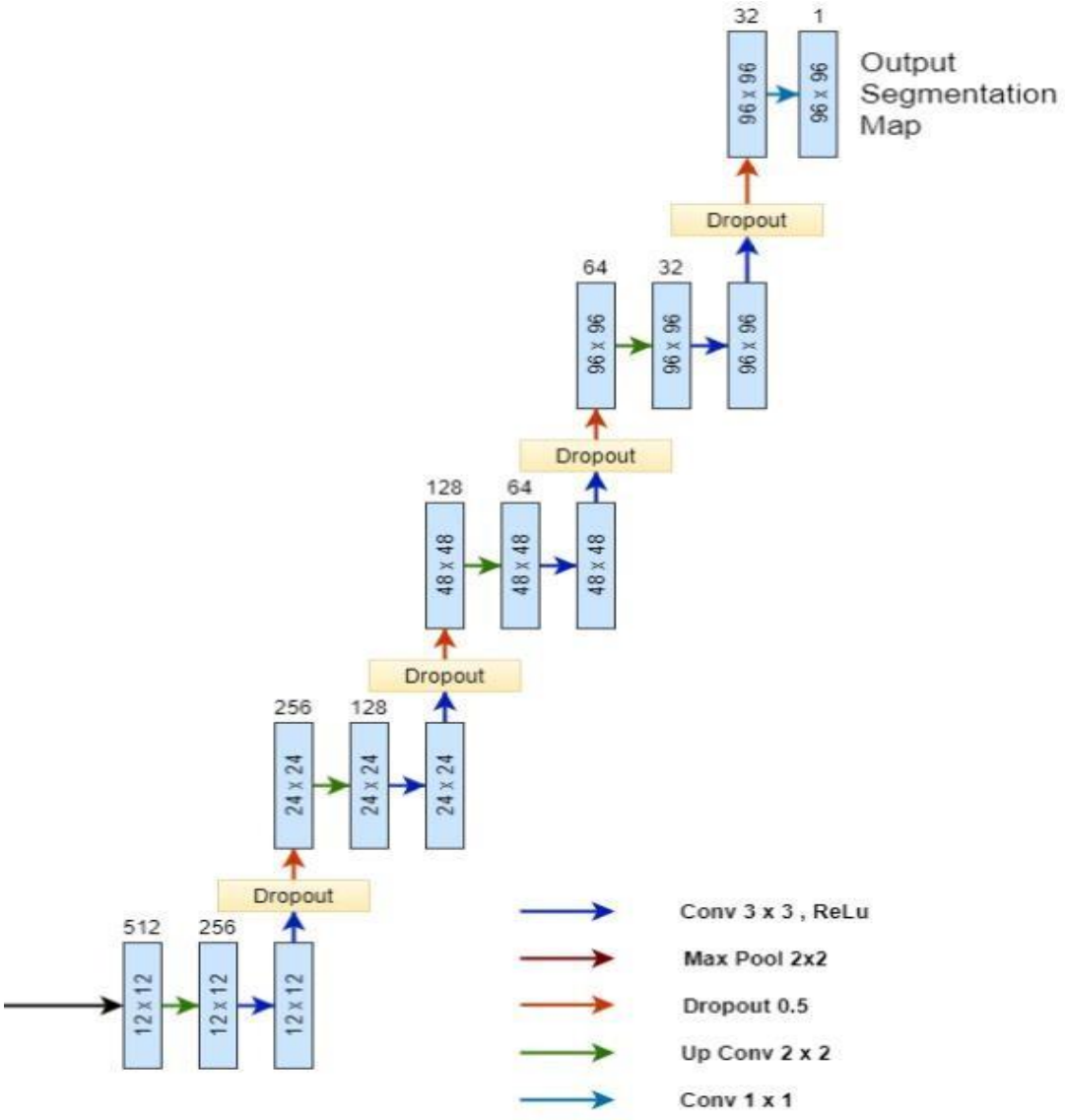

Figure 6.4: Decoder Pipeline of Tsallis-UNet Model

6.4.2 Tsallis Entropy Pooling Pipeline

This is the half where Tsallis Entropy is implemented. It begins at 4^{th} layer of encoder. The information retained by the feature maps from the training image is transformed in this half which is then fed to a dense-net and compared with the true image labels that were created during the preprocessing.

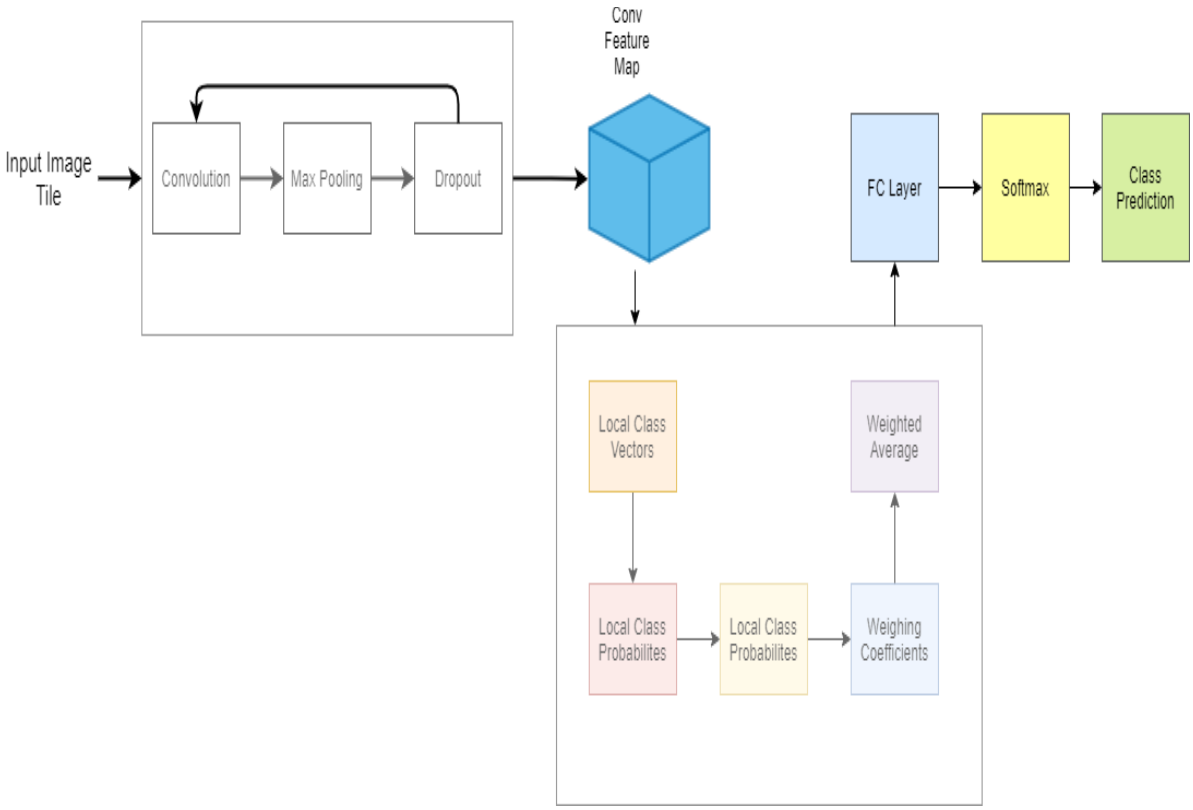

Figure 6.5: Tsallis Entropy Pooling pipeline of
Tsallis-UNet Model

This pipeline has drawn inspiration from a typical CNN architecture which consists of several convolutional layers, a GAP layer and finally a classifier which is usually a FC layer. Let be the global averaging operation on the classification score vector, where $U \varepsilon R^{h \times wxc} \cdot U$consists of local class prediction vectors.

The GAP layer used to perform a simple averaging operation is:

$$f_G(U) = \frac{1}{hw} \sum_i v_i \tag{4}$$

Equation (4) as per 4, is not optimum as it forces the model to focus on every image region with equal priority, hence the model is

more prone to distraction during training. Hence Tsallis Entropy is employed to replace equation (4).

The 4th Layer of Encoder gives a feature map of size 12 x 12 x 256. For each of the 256 feature maps, any region $i \ \varepsilon \ [1, 144]$ in the image let the pixel value be v_i. Therefore, it can be concluded that any v_i which gives lower entropy must be given higher priority in training. Following this theory $p_i = SoftMax(v_i)$ is calculated as local class probability. After this Tsallis Entropy for each i is calculated as per Equation (2) or Equation (1) depending on the entropic index(q) value assumed for the system.

Let λ_i be the weight coefficient for local class prediction v_i. Since λ_i is negatively correlated to the Tsallis Entropy it can be formulated as:

$$\lambda_i = 1 - \frac{S_i(p_i)}{\max\limits_{j\varepsilon(1,hw)} S_j(p_j)} \tag{5}$$

Finally, each weight coefficient is multiplied with its corresponding v_i and given to Averaging Layer.

The Average calculated in Equation (6) is more balanced with respect to noise when compared with Equation (4). It gives the right amount of priority to each of the image region based on the noise.

Above process is repeated for each of the feature maps and thus we get 256 average values. These values are flattened and fed into a Fully Connected Neural Network (FCNN) that has one hidden layer of 32 nodes with ReLu activation and an output layer of 1 node with SoftMax activation. This layer predicts if Brachial Plexus Nerve is present in the US image. The result is then compared with training labels created during the pre-processing.

6.5 Training of Model

Prior to runtime the entire training dataset is divided into 32 batches with a 80:20 ratio where 80% is used for training and the remaining 20% is used for validation and run for 20 epochs.

Optimizer used for both the models will be Adam optimizer with a learning rate of 0.00001. For Model A loss function used is Dice Coefficient. For Model B Dice Coefficient Loss function is used by Decoder Pipeline whereas Binary Cross Entropy Loss is used by Tsallis Pipeline.

6.5.1 Dice Coefficient Loss Function

Dice Loss Score is one of the most common loss score used for image segmentation. It provides a direct comparison between a annotated ground truth S_{gt} and predicted truth value S_{pred} as follow

$$\frac{2|s_{gt}+s_{pred}|}{|s_{gt}|+|s_{pred}|} = \frac{2TP}{2TP+FP+FN}$$

It does consider True Positives in higher regards to other values, however, if it encounters False Negatives then the score value can get skewed thus affecting the training model. But overall the score value is very robust.

6.5.2 Binary Cross Entropy Loss Function

This loss function works well for Tsallis pipeline of Model B which gives output in either of the two class that is 0 and 1. The loss function is defined as follows:

$$H_p(q) = \frac{-1}{N} \sum_{i=1}^{N} y_i \, log(p(y_i)) + (1 - y_i) \, log(1 - p(y_i))$$

6.5.3 Selection of Appropriate Loss Metric

Model B relies on two different loss functions as compared to Model A which only relies on one. As a result, in order to compare the performance of the two model we need to have a loss metric that is mutual for both.

We cannot rely on Dice Coefficient Loss even though it is common to both the models. This is because in the two-header approach of Model B, training of weights in the encoder half is going to be done based on the combine error from both its loss functions. Hence the loss score of one

function in the previous batch will indirectly affect the loss score of the other function in the next batch. This makes Dice Score less effective metric for comparison of the two model.

We cannot rely on Accuracy metric. This accuracy metric works well for image classification problems where the metric's value indicates the quantity of data that has been correctly classified. Since Image Segmentation is pixel will classification, we require much finer metric for comparison. Also monitoring the training of the model solely based on the Training Loss value may improve its accuracy for training set but it can greatly skew the results for validation set, thereby risking the model to highly overfit on the data.

In conclusion the most reliable metric is **Validation Loss Score**. Unlike Accuracy metric, it gives finer information regarding pixel wise classification for a batch. Monitoring validation loss during training reduces the likeliness of overfitting or underfitting of model.

Chapter 7

Results and Discussion

7.1 Training of Model A

Training of Model A was straight forward. After fixing batch size, epochs and other parameters as mentioned in section 6.5, the validation loss stood out to be **0.69273**

7.2 Training of Model B

Since Model B has entropic index q as an additional hyperparameter, the training process is divided into two segments- one to decide the nature of the datasets and the other to locate an optimum range for q.

7.2.1 Training of Model B to compare with Model A

Since Model B is integrated with Tsallis, it becomes crucial to decide whether the model is sub-extensive, extensive or super-extensive. In order to achieve a conclusion, 7 equally placed hyperparameters is selected starting from 0.25 with an increment of 0.25. Thus, the model is trained with 0.25,0.50,0.75,1.00,1.25,1.50 and 1.75 as q.

Table 7.1: Validation Loss variation with respect to q at increment rate 0.25

Hyperparameter in Tsallis-UNET	**Validation Loss**
0.25	0.39140
0.50	0.39375
0.75	0.43505

1.0	0.41463
1.25	0.36531
1.5	0.36428
1.75	0.37742

From table 7.1 it is observed that the model faces a sharp drop in validation loss when trained for entropic index $q > 1$. The model is indicated to be less distracted by noise at $q > 1$ and preforms better when considered to have super-extensive properties.

From table 7.1 it is also inferred that Model B performs better than Model A by the fact that presence of any value of entropic index q reduces the loss score.

7.2.2 Training of Model B to locate optimum entropic index

From table {mention previous table} it is observed that model loss is minimized for q in range of 1.25 and 1.75. This training is carried out to locate an optimum value of q for the given dataset. This is done in a two-fold approach. In the first fold, q is varied from 1.25 to 1.75 with an increment rate of 0.05.

Table 7.2: Validation Loss variation with respect to q at increment rate 0.05

Hyperparameter in UNET	**Validation Loss**
1.25	0.36531
1.30	0.35025
1.35	0.35930
1.40	0.36634
1.45	0.36979
1.50	0.36428
1.55	0.37358
1.60	0.37159

1.65	0.37180
1.70	0.37658
1.75	0.37742

From table 7.2 it is observed that validation loss shows a drop for *q* in range 1.25 to 1.35. In the second fold, *q* is varied from 1.25 to 1.35 with an increment rate of 0.01.

Table 7.3: Validation Loss variation with respect to q at increment rate 0.01

Hyperparameter in UNET	**Validation Loss**
1.25	0.36531
1.26	0.36420
1.27	0.36105
1.28	0.35756
1.29	0.35143
1.30	0.35025
1.31	0.32884
1.32	0.35074
1.33	0.35123
1.34	0.35578
1.35	0.35930

From table 7.3 it is inferred that the model minimizes the validation loss to 0.32884 at $q = 1.31$.

This two-fold approach is necessary as it showed that the optimum *q* range for any dataset similar to the US image dataset is [1.25,1.35]. For this specific dataset the optimum q is 1.31. Even though the change in loss is very small for q in [1.25,1.35], in field of medical image segmentation this small change has greatly improved the overall performance of model in giving more accurate predicted masks.

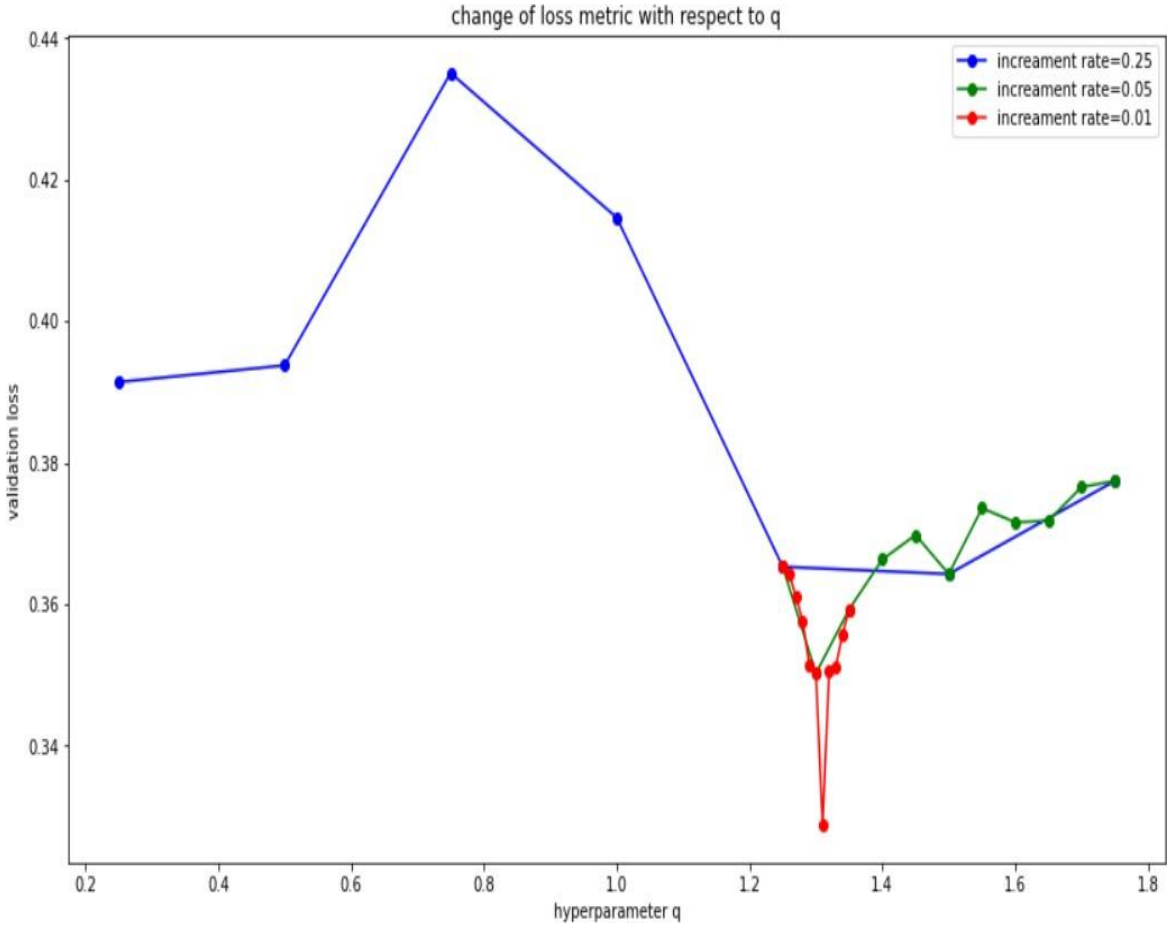

Figure 7.1: Convergence to optimum entropic index

Chapter 8

Conclusion and Future Work

8.1 Conclusion

This project has explored the segmentation of Brachial Plexus nerves from ultrasound images using a deep convolution neural network. In this project we have studied the working of Base UNet model and have integrated and implemented Tsallis Entropy into it. Training Results have shown that Tsallis-UNet performs better than Base-UNet in terms of preventing noise distraction and producing accurate results. The project has discovered the extensivity of the dataset. It has explored the performance of the new model with respect to the change in entropic index and has given a convincing range for the hyperparameter which can be used for further such models when dealing with similar low intensity-low contrast US datasets.

8.2 Future Work

There are several aspects where we can still do further research:

1. Creating a sophisticated post-processing technique which would enhance the low image quality of predicted masks.
2. Creating a dynamic model augmented with Ultrasound devices that would continuously generate ROI in ultrasound sonography in real time without inducing much computational overhead on the said device.

Chapter 9

References

1. *A. Kakade and J. Dumbali, "Identification of nerve in ultrasound images using u-net architecture," in 2018 International Conference on Communication information and Computing Technology (ICCICT). IEEE, 2018, pp. 1–6.*

2. *O. Hadjerci, A. Hafiane, P. Makris, D. Conte, P. Vieyres, and A. Delbos, "Nerve detection in ultrasound images using median gabor binary pattern," in International Conference Image Analysis and Recognition. Springer, 2014, pp. 132–140.*

3. *B. Kayalibay, G. Jensen, and P. van der Smagt, "Cnn-based segmentation of medical imaging data," arXiv preprint arXiv:1701.03056, 2017.*

4. *R. J. Cunningham, P. J. Harding, and I. D. Loram, "Real-time ultrasound segmentation, analysis and visualisation of deep cervical muscle structure," IEEE transactions on medical imaging, vol. 36, no. 2, pp. 653–665, 2017.*

5. *M. Baby and A. Jereesh, "Automatic nerve segmentation of ultrasound images," in Electronics, Communication and Aerospace Technology (ICECA), 2017 International conference of, vol. 1. IEEE, 2017, pp. 107–112.*

6. *M. Portes de Albuquerque, I.A. Esquef and A.R. Gesualdi Mello, "Image Thresholding using Tsallis Enrtopy," in Pattern Recognition Letters 25 (2004) 1059-1065.*

7. *O. Ronneberger, P. Fischer, and T. Brox, "U-net: Convolutional networks for biomedical image segmentation," in International Conference on Medical Image Computing and Computer-Assisted Intervention. Springer, 2015, pp. 234–241.*

8. *J. Long, E. Shelhamer, and T. Darrell, "Fully convolutional networks for semantic segmentation," in Proceedings of the IEEE Conference on Computer Vision and Pattern Recognition, 2015, pp. 3431–3440.*

9. *Y. Li. Segmentation of medical ultrasound images using convolutional neural networks with noisy activating functions.*

10. *C. Azzopardi, Y. A. Hicks, and K. P. Camilleri, "Automatic carotid ultrasound segmentation using deep convolutional neural networks and phase congruency maps," in Biomedical Imaging (ISBI 2017), 2017 IEEE 14th International Symposium on. IEEE, 2017, pp. 624–628.*

11. *H. A. Nugroho, M. Ramaswamy, Y. Triyani, and I. Ardiyanto, "Neutrosophic and fuzzy c-means clustering for breast ultrasound image segmentation," in Information Technology and Electrical Engineering (ICITEE), 2017 9th International Conference on. IEEE, 2017, pp. 1–5.*

12. *J. J. Cerrolaza, M. Sinclair, Y. Li, A. Gomez, E. Ferrante, J. Matthew, C. Gupta, C. L. Knight, and D. Rueckert, "Deep learning with ultrasound physics for fetal skull segmentation," in Biomedical Imaging (ISBI 2018), 2018 IEEE 15th International Symposium on. IEEE, 2018, pp. 564–567.*

13. *Z. Zhang, M. Tang, D. Cobzas, D. Zonoobi, M. Jagersand, and J. L. Jaremko, "End-to-end detection-segmentation network with roi convolution," IEEE 15th International Symposium on Biomedical Imaging, 2018.*

14. *Kaggle ultrasound nerve segmentation. [Online]. Available: https://www.kaggle.com/c/ultrasound-nerve-segmentation.*

15. *R. Mehta and J. Sivaswamy, "M-net: A convolutional neural network for deep brain structure segmentation," in Biomedical Imaging (ISBI 2017), 2017 IEEE 14th International Symposium on. IEEE, 2017, pp. 437–440. 16.12 .2009.*